Published in final edited form as:
Exp Cell Res. 2013 July 15; 319(12): 1828–1838. doi:10.1016/j.yexcr.2013.03.025.

On the role of 25-hydroxycholesterol synthesis by glioblastoma cell lines. Implications for chemotactic monocyte recruitment

Gerald Eibinger[a], **Günter Fauler**[b], **Eva Bernhart**[a], **Sasa Frank**[a], **Astrid Hammer**[c], **Andrea Wintersperger**[a], **Hans Eder**[d], **Akos Heinemann**[e], **Paul S. Mischel**[f], **Ernst Malle**[a], and **Wolfgang Sattler**[a,*]

[a]Institute of Molecular Biology and Biochemistry, Medical University of Graz, Harrachgasse 21, Graz 8010, Austria

[b]Clinical Institute of Medical and Chemical Laboratory Diagnostics, Medical University of Graz, Graz 8010, Austria

[c]Institute of Cell Biology, Histology and Embryology, Medical University of Graz, Graz 8010, Austria

[d]Department of Neurosurgery, Medical University of Graz, Graz 8010, Austria

[e]Institute of Experimental and Clinical Pharmacology, Medical University of Graz, Graz 8010, Austria

[f]Ludwig Institute for Cancer Research, La Jolla, California, CA 92093, USA

Abstract

Glioblastoma multiforme (GBM) is the most common malignant primary brain tumor and is invariably fatal to affected patients. Oxysterols belong to a class of bioactive lipids that are implicated in neurological disease and are associated with various types of cancer. Here, we investigated expression and transcriptional regulation of cholesterol 25-hydroxylase (CH25H) in human U87MG and GM133 glioblastoma cell lines. We demonstrate that in both cell lines transcription and translation of CH25H are increased in response to TNFα and IL1β. In parallel, both cell lines upregulate 25-hydroxycholesterol (25-OHC) synthesis and secretion to levels comparable to bone marrow-derived mouse macrophages under inflammatory conditions. To determine whether 25-OHC acts as chemoattractant for tumor-associated macrophages, the human THP-1 monoblastic leukemia cell line was treated with varying amounts of the oxysterol. Experiments revealed that 25-OHC and lipid extracts isolated from GM133-conditioned medium (containing 7-fold higher 25-OHC concentrations than U87MG medium) induce chemotactic migration of THP-1 cells. Of note, 25-OHC also induced the migration of primary human peripheral blood monocytes. In response to exogenously added 25-OHC, THP-1 cells reorganized intermediate filament-associated vimentin to more cortical and polarized structures. Chemotactic migration of monocytes in response to 25-OHC was pertussis toxin-sensitive, indicating the involvement of G protein-coupled receptors. Using RNA interference we demonstrated that G protein–coupled receptor 183 (EBI2) contributes to 25-OHC-mediated chemotactic migration of

*Corresponding author. Fax: +43 316 380 9615. wolfgang.sattler@medunigraz.at (W. Sattler) .

Europe PMC Funders Author Manuscripts

THP-1 cells. These in vitro data indicate that GBM-derived and secreted 25-OHC may be involved in the recruitment of immune-competent cells to a tumor via EBI2.

Keywords

EBI2; Migration; Glioblastoma; TNFα; IL1β

Europe PMC Funders Author Manuscripts

Introduction

Oxysterols are hydroxylated derivatives of cholesterol that play important functions in lipid metabolism and, as signaling-active and mutagenic compounds, received considerable attention in tumor biology [1]. A number of studies revealed that there is no net movement of cholesterol from the peripheral circulation into the CNS and there is general agreement that the brain covers its cholesterol demand by endogenous biosynthesis [2]. Excess brain cholesterol is hydroxylated mainly to 24S-hydroxycholesterol (24S-OHC) and secreted via the blood–brain barrier into the circulation [2]. 24S-OHC is transported in association with lipoproteins and metabolized by the liver [2]. Alternatively, 24S-OHC acts as a bioactive oxysterol in the brain regulating the expression of enzymes involved in cholesterol homeostasis [3]. Apart from 24S-OHC the brain is capable of synthesizing, besides 27-OHC via CYP27A1, 25-OHC via cholesterol 25-hydroxylase (CH25H).

CH25H is inducible by interferons [4] and 25-OHC concentrations are elevated in humans exposed to endotoxin treatment [5]. Two distinct receptor families are represented among the effectors that are known to bind oxysterols, namely the nuclear receptor transcription factors and G protein-coupled seven transmembrane domain receptors. Consequently oxysterols are able to interfere with tumor growth in a dual manner: (i) through regulation of the proinflammatory potential of immune cells by dampening the anti-tumor response of dendritic cells in an liverXreceptor (LXR) dependent manner [6] or (ii) by recruiting a population of (pro-tumorigenic) immune cells via LXR-independent pathways [7].

25-OHC is a potent regulator of LXR-mediated pathways, that impact on brain lipid homeostasis [8]. This oxysterol affects expression of the cholesterol efflux pumps ATP-binding cassette transporter (ABC)A1 [9] and ABCG1, and expression of apolipoprotein E [10–12]. 25-OHC is able to stimulate LXR-independent oligodendrocyte apoptosis and suppresses myelin gene expression in peripheral nerves via LXR/Wnt/β-catenin-mediated pathways [13]. LXR-mediated pathways interfere with cholesterol metabolism and, therefore, it is not surprising that oxysterols in the micromolar range are able to inhibit cancer cell proliferation including glioblastoma [14], breast [15] and prostate cancer cells [16] as well as prostate cancer xenografts [17]. LXR agonists interfere with several cell cycle checkpoints inducing cell cycle arrest and phytosterols (plant LXR agonists) were suggested to reduce the incidence of colon cancer [18]. 25-OHC can further act as a negative regulator of sterol regulatory element binding protein (SREBP)-dependent pathways by binding to insulin-induced gene 1 and 2 anchor proteins (Insig1 and -2) thereby inhibiting proteolytic activation of SREBPs [19].

In vitro studies further demonstrated that 20(S)-OHC may also interact with membrane receptors, activating the Hedgehog signaling pathway via binding to the oncoprotein Smoothened [20]. In a similar manner 25-OHC promotes medulloblastoma growth via activation of the Sonic Hedgehog pathway [21]. Conversion of 25-OHC to the more polar 25-OHC-3-sulfate by tumor cells decreases LXR affinity and exerts LXR antagonistic properties via peroxisome proliferator activated receptor (PPAR) γ activation [22] leading to increased tumor cell growth and tumor immune escape [23].

Glioblastoma multiforme (GBM; astrocytoma grade IV) is the most common and malign primary brain tumor with a mean survival of 14.6 months even under current maximal therapy including surgery and combined chemo- and radiotherapy [24]. Only recently it was demonstrated that the mutated epidermal growth factor receptor (EGFR) present in a high percentage of GBMs overcomes normal cell regulatory mechanisms to feed large amounts of cholesterol to brain cancer cells [13]. We have shown that EGFRvIII upregulates SREBP1 cleavage [25] and low-density lipoprotein receptor expression, thereby promoting cholesterol uptake, which favors growth and survival of GBM cells [14]. This pathway, which renders tumor cells exquisitely sensitive to LXR agonist-mediated apoptosis [13], could also feed excess cholesterol into the oxysterol synthesis pathways.

Oxysterols modulate the immune responses and as such could be effectors of the tumor environment: 25-OHC impairs IgA production in B-lymphocytes [26] and induces the secretion of the proinflammatory and angiogenic cytokine IL-8 [27,28]. Of note, oxysterols (in particular 7α,25-OHC) are potent chemoattractants for immune cells via Epstein-Barr virus-induced G protein-coupled receptor 2 (EBI2; also termed GPR183) [29,30]. Besides regulating normal function of the immune system this pathway might be of importance in the tumor environment, contributing to chemotactic recruitment of monocytes across the tumor vasculature and subsequent deposition of tumor-associated macrophages.

The present study aimed at investigating CH25H expression on mRNA and protein level in two GBM cell lines with different in silico CH25H mRNA expression (http://biogps.org). We explored the effects of TNFα and IL-1β (cytokines secreted by GBM cells [31–33]) on CH25H transcription and translation, and quantitated its product 25-OHC by GC–MS analysis. Using THP-1 and primary human blood monocytes we studied the effects of exogenous 25-OHC and GBM-conditioned medium on cell migration, since monocyte-derived macrophages are known to contribute to increased aggressiveness and invasiveness of glioblastoma [34]. Finally, the involvement of the G protein-coupled receptor EBI2 in 25-OHC-mediated migration of THP-1 cells was investigated.

Materials and methods

Materials

25-OHC and all standard solvents were from Sigma (Vienna, Austria). Deuterated (26,26,26,27,27,27-D_6-)25-OHC was from Dr. Ehrenstorfer GMBH (Augsburg, Germany). Cell culture supplies, TNFα and IL1β were from Gibco (Invitrogen, Vienna) or PAA Laboratories (Linz, Austria). Recombinant MCP-1 was from Pepro-Tech (Rocky Hill, NJ, USA).

The following antibodies were used: Monoclonal mouse-anti CH25H [26], the rabbit polyclonal antibody against calnexin was from Santa Cruz Biotechnology (CA, USA), and the rabbit polyclonal antibody against EBI2 was from LSBiosciences (WA, USA). HRP-labelled goat anti-mouse IgG was from Santa Cruz Biotechnology and HRP-labelled goat anti-rabbit IgG was from Pierce (Thermo Scientific, MA, USA). Mouse anti-human vimentin, blocking solution and antibody diluent was from DAKO (Jena, Germany). Cyanine-3 (Cy3) goat-anti mouse antibody was from Jackson laboratories (Bar Harbour, ME, USA) and DAPI solution was from Partec (Münster, Germany).

BCA protein assay kit and SuperSignal Western blot detection reagent kit were from Pierce (Thermo Scientific, MA, USA) and ECL Plus Western Blotting Reagents were form Amersham Biosciences (Vienna). SuperScript II Reverse Transcriptase was from Invitrogen (Vienna). Random hexamer primer was from Thermo Scientific (MA, USA). RNeasy Plus Kit, QuantiFast SYBR Green PCR kit, QuantiTect primer assays Cholesterol-25-hydroxylase (Hs_CH25H_1_SG), G protein-coupled-receptor 183 (Hs_EBI2_1_SG), Hydroxymethylbilanesynthase (Hs_HMBS_1_SG), Glyceraldehyde-3-phosphate-dehydrogenase (Hs_GAPDH_2_SG) and the siRNAs targeting EBI2 were from Qiagen (Hilden, Germany). Non-targeting siRNA (scrambled siRNA) was from Dharmacon (Thermo Scientific). GenMute transfection reagent was from SignaGen laboratories (MD, USA). Transwell plates with 8.0 μm polycarbonate membrane inserts (24-well plates) for cell migration experiments were from Costar (Vienna).

Cell culture

U87MG and GM133 cells were cultured in DMEM medium (Invitrogen) with 10% (v/v) FCS and penicillin/streptomycin (Invitrogen). GM133 cells are derived from a glioblastoma patient biopsy; their culture has been previously described in detail [35]. Before use for experiments cells were kept under serum-free conditions for at least 4 h. The only exception was oxysterol efflux experiments, where FCS was used as lipid acceptor. Cytokine stimulation was performed with TNFα (0.3 ng/ml to 30 ng/ml) or IL1β (0.05 ng/ml to 5 ng/ml).

RT-qPCR

RNA was extracted using an RNA Extraction Kit (Qiagen) according to manufacturer's suggestions. Before reverse transcription, RNA concentration was determined by a Nanodrop ND-1000 spectrophotometer (Peqlab). One to three μg of RNA were used for reverse transcription, which was performed with the Super-Script II Reverse Transcription Kit and random hexamer primers (Invitrogen) according to manufacturer's protocol. The temperature profile was: 25 °C for 10 min, 42 °C for 50 min and 70 °C for 15 min. Real-time analysis was performed using SyBr Green PCR kit and Quantitec primer assays (Qiagen) according to manufacturer's protocol with a 7900 Fast Real-Time-PCR-System (Applied Biosciences). GAPDH and HMBS were used as housekeeping genes. The following primers were used: CH25H (Hs_CH25H_1_SG), EBI2 (Hs_EBI2_1_SG), GAPDH (Hs_GAPDH_2_SG) and HMBS (Hs_HMBS_1_SG). Statistical analyses of qPCR analyses were performed using the REST software (http://www.gene-quantification.de; Ref. [36]).

Western blotting

Cells were lysed with 50 µl Ripa buffer (50 mM Tris–HCl, 1% (v/v) Nonoxinol 40, 150 mM NaCl, 1 mM Na_3VO_4, 1 mM NaF and 1 mM EDTA) containing protease inhibitors and PMSF. The lysate was kept on ice for 10 min, centrifuged with 10,000 × *g* for 10 min and the supernatant was collected. Protein content was measured by BCA protein assay kit according to manufacturer's protocol. Proteins were separated by SDS-PAGE (12%; 150 V, 1.5 h) and transferred to PVDF membranes (150 mA, 1 h). CH25H was detected using a monoclonal antibody, calnexin and EBI2 were detected with polyclonal rabbit antibodies; both antibodies were diluted 1:1000 in antibody diluent. Immunoreactive bands were visualized using HRP-conjugated secondary antibodies and subsequent ECL Plus development. Luminescence was detected using a ChemiDocMP system (BioRad) followed by analysis with the ImageLab software (BioRad).

Lipid extraction

U87MG or GM133 cells were seeded on 10 cm Petri dishes and grown to 70–80% confluence. Cells were treated with cytokines at the indicated concentrations for 24 h. Thereafter, medium was collected and centrifuged to remove remaining cells. Cells were washed twice with PBS and scraped with 200 µl PBS. Twenty ng D_6-25-OHC (MW=408.69 Da) was added as internal standard. Lipid extraction was performed according to Folch [37]. In brief, lipids were hydrolyzed in ethanolic KOH; after neutralization with acetic acid and addition of NaCl (200 µmol per extraction) lipids were extracted (twice) with chloroform/methanol (2:1; v/v). The chloroform phases were collected and dried under a gentle stream of nitrogen. The dried lipids were derivatized with MSTFA/pyridine (2:1; v/v) containing 1% (v/v) TMCS at 37 °C for 30 min.

Gas chromatography-mass spectroscopy (GC–MS) analysis

A Fisons model 8000 gas chromatograph, equipped with a HT5 fused silica capillary column (25 m × 0.22 mm i.d., 0.1 µm film thickness) from SGE (SGE Analytical Science, Griesheim, Germany), coupled to a Fisons MD 800 quadrupol mass spectrometer, was used for detection. The splitless Grob-injector was kept at 220 °C. Helium was used as carrier gas with a constant flow of 1 ml/min. The initial column temperature of 200 °C was held for 1 min and followed by an increase of 15 °C/min to 280 °C, a hold at 280 °C for 10 min, followed by an increase of 15 °C/min to 300 °C and a final isothermal hold of 7 min. The connection between GC and MS instrument was kept at 300 °C. The ion source temperature was 200 °C. Mass spectra were recorded with electron ionization energy of 70 eV and an emission current of 100 µA. The diagnostic ions used for (two-fold) silylated 25-OHC were at *m/z*=131.1, 456.4 und 546.4. Silylated D_6-25-OHC was detected at *m/z*=137.1, 462.4 and 552.4.

Preparation of GM133-conditioned medium extract

GM133 cells were seeded in a 75 cm^2 flask and grown until 80% confluence. Fresh medium (10 ml) was added and kept on the cells for 2 days. Medium lipid extraction was performed as described above. After drying under nitrogen, lipid extracts were reconstituted in 30 µl

ethanol. For migration experiments 0.5 µl (per 500 µl RPMI medium containing 0.1% (w/v) BSA, see below) of this solution was used.

Cell migration

Non-differentiated THP-1 cells (grown in suspension in RPMI medium containing 10% FCS) were centrifuged and resuspended in serum-free RPMI medium. Cell number was determined using a Bürker-Türk hemocytometer and 100,000 cells (in 100 µl) were seeded into the upper chamber of a 6.5 mm Transwell chamber (Corning) with 8.0 µm pore size. For migration of human blood monocytes, 500,000 cells were seeded in serum-free RPMI medium into the upper Transwell compartment. The lower chamber was filled with 500 µl RPMI medium containing 0.1 (w/v)% BSA (as an oxysterol acceptor), vehicle (0.1% ethanol; v/v), FCS (5%), MCP-1 (50 ng/ml), 25-OHC (2.5 nM, 25 nM, 75 nM, or 150 nM), or GM133-conditioned medium extract (0.5 µl/500 µl medium). Pertussis toxin (PTX; 30 ng/ml) was added to the upper chamber before starting the experiment. After 4 (primary human blood monocytes) or 18 h (THP-1) the number of transmigrated cells in the lower chamber was determined by counting at least nine large squares per sample and normalized to the vehicle-containing (0.1% BSA, 0.1% ethanol) control. Chemokinesis experiments were performed with equal amounts of agonists in the top and bottom wells as described [38].

Isolation of human peripheral blood monocytes

Blood was obtained after written informed consent from healthy normal subjects, as approved by the Institutional Review Board of the Medical University of Graz. Donors were taking no systemic medication and were showing normal values of C-reactive protein. Citrated blood (40 ml) was centrifuged at 300 × *g* for 20 min (room temperature) to remove platelet-rich plasma and erythrocytes as described [39]. For separation of polymorphonuclear leukocytes (containing neutrophils and eosinophils) from peripheral blood mononuclear cells (comprising monocytes and lymphocytes), the supernatant was layered on 15 ml Histopaque (1077 Density, Sigma). After centrifugation (350 × *g* for 20 min) the mononuclear cells of the interface were removed, washed with PBS containing 5.5 mM glucose and 2.7 mM KCl. Monocytes were then purified by negative magnetic selection using an antibody cocktail from Miltenyi (Bergisch Gladbach, Germany), yielding 95% monocytes with 99% viability. Monocytes were resuspended in RPMI 1640 supplemented with penicillin, streptomycin, glutamine (20 mM), non-essential amino acids, HEPES 0.05 M and sodium pyruvat 10 mM and counted.

Immunofluorescence

Cells were centrifuged onto glass slides by a Cytospin 2 centrifuge (Shandon), dried for 20 min and stored at −20 °C until experimental use. Then cells were fixed with acetone for 5 min and dried for 30 min, and treated with blocking solution (DAKO) for 10 min. The anti-vimentin antibody (DAKO) was diluted 1:50 in antibody diluent (DAKO) and kept on the cells in a humidified chamber for 45 min. Slides were rinsed 5 times in PBS and incubated with Cy3-labeled goat anti-mouse (dilution 1:300, 30 min). Finally, the slides were counterstained with DAPI (Partec; 1:500, 5 min) rinsed 3 times in distilled water and

covered with Moviol and a cover slip. Microscopy was performed on a confocal laser-scanning microscope (Leica SP2, Leica Lasertechnik GMBH, Heidelberg, Germany) using 543 nm excitation wavelength for Cy3 and 405 nm for DAPI. Detected emission wavelength were 555 nm to 620 nm for Cy3 and 430 nm to 450 nm for DAPI.

siRNA transfection

THP-1 cells (400,000) were seeded into a 6-well plate and transfected with 40 picomoles of EBI2 siRNA (Qiagen) (a mixture of 10 picomoles Hs_EBI2_1, Hs_EBI2_3, Hs_EBI2_4 and Hs_EBI2_5, respectively) or scrambled siRNA using GenMute transfection reagent according to the manufacturer's suggestions. Forty eight hours post transfection migration experiments, RT-PCR, or Western blotting experiments were performed as described above.

Statistical analysis

Statistical analysis was performed using the GraphPad Prism 5 software. For determination of statistical significance unpaired two-tailed *t*-test and one tailed ANOVA with or without Bonferroni post-hoc test were used. p values<0.05 were considered statistically significant.

Results

CH25H mRNA and protein expression by U87MG and GM133 glioblastoma cells is induced by proinflammatory cytokines

As cytokines act as important modulators of the tumor environment [40] their effect on CH25H expression in both glioblastoma cell lines was investigated. Exogenously added TNFα resulted in significant upregulation of CH25H mRNA levels (2.1-, 7.2- and 11-fold at 0.3 ng/ml, 3.0 ng/ml and 30 ng/ml, respectively) in U87MG cells (Fig. 1A). In contrast, IL1β had less pronounced effects on CH25H mRNA expression reaching a maximum induction of 4.5-fold (Fig. 1B). Increased CH25H mRNA expression in response to TNFα was accompanied by increased expression of CH25H protein (Fig. 1C).

In silico analysis using BioGPS (http://biogps.org) revealed that the glioblastoma cell line GM133 shows highest CH25H expres sion among all cancer cells included in the NCI-60 dataset. Stimulation of GM133 cells with TNFα resulted in a maximum increase of mRNA expression by 5-fold (Fig. 1D). In contrast, IL1β was more efficient with regards to transcriptional regulation of CH25H by increasing mRNA levels up to 10-fold at the highest cytokine concentrations used (Fig. 1E). Also protein levels of CH25H were increased in response to IL1β (Fig. 1F) to higher levels as found in U87MG cells (Fig. 1C).

TNFα and IL1β increase 25-OHC synthesis and secretion in U87MG and GM133 cells

The next set of experiments aimed to clarify whether upregulated CH25H mRNA and protein expression is accompanied by increased product generation. Cellular and medium lipid extracts of TNFα and IL1β-treated glioblastoma cells were analyzed by GC–MS as the corresponding trimethylsilyl (TMS)-derivatives. Selected ion-monitoring traces of TMS-derivatives of 25-OHC (analyzed from GM133 cellular lipid extracts; diagnostic ions at m/z=131.1) and D_6-25-OHC (m/z=137.1; internal standard) are shown in Fig. 2A and B. Full scan electron impact (EI) spectra for TMS-derivatives of 25-OHC and D_6-25-OHC are

shown in Fig. 2C and D. The proposed fragmentation patterns for both analytes are shown as insets in Fig. 2C and D.

Subsequently, product formation was analyzed in response to the cytokine that showed highest efficacy in terms of CH25H expression (Fig. 1). Intracellular 25-OHC concentrations in U87MG cells increased from 9.9 ng/mg to 15 ng/mg cell protein in response to TNFα (Fig. 3). Concentrations of secreted 25-OHC increased significantly ($p<0.005$) from 5.8 ng/mg to 18 ng/mg cell protein. In line with high mRNA and protein levels of CH25H in GM133 cells (Fig. 1) cellular and medium 25-OHC concentrations under basal conditions were 10- to 30-fold higher as compared to U87MG cells. Exogenously added IL1β led to a further increase from 66 ng/mg to 95 ng/mg cell protein ($p<0.005$) while extracellular 25-OHC concentrations increased from 160 ng/mg to 300 ng/mg cell protein (Fig. 3).

25-OHC induces chemotactic migration of THP-1 cells

Next we examined whether 25-OHC exerts direct effects on chemotactic migration of human THP-1 monocytes used as model cell line for tumor-associated macrophages. 25-OHC added to the lower chamber led to increased transmigration (1.3-, 1.4- and 1.3-fold at 2.5 nM, 25 nM and 75 nM 25-OHC, respectively; Fig. 4A) of cells across uncoated Transwell inserts. To differentiate between chemotaxis and chemokinesis, 25-OHC was added only to the lower (chemotaxis) or to the upper and lower (chemokinesis) chamber of Transwell chambers. These experiments revealed that 25-OHC induces THP-1 migration only when present in the lower compartment, indicating that 25-OHC acts as chemotactic agent (Fig. 4B). 25-OHC added to the lower and upper compartment was without effect on migration (Fig. 4B). However, the chemotactic potential of 25-OHC was lower as compared to monocyte chemotactic protein-1 (MCP-1; Fig. 4B). Of note, 25-OHC was also able to increase migration of primary human peripheral blood monocytes between 1.4- and 1.6-fold (75 nM and 150 nM 25-OHC) in comparison to untreated cells (Fig. 4C).

To get an indication whether the migratory effects are accompanied by changes in the intermediate filaments of the THP-1 cell cytoskeleton, vimentin, an important regulatory protein of cell motility, was visualized by immunofluorescence microscopy. As shown in Fig. 5, exogenously added 25-OHC changed the vimentin intermediate filament architecture in THP-1 cells from a cytoplasmic distribution to a more cortical location with multiple extensions, indicative of monocyte polarization in response to 25-OHC (Fig. 5; arrows).

Given the rather efficient secretion of 25-OHC in the cellular supernatant of GM133 cells we reasoned that lipid extracts prepared from conditioned GM133 medium would affect THP-1 migration. Lipid extracts were reconstituted in ethanol and added to medium to result in a 25-OHC concentration of approx. 25 nM. These experiments revealed that the medium lipid extracts from GM133 cells promote migration to a similar extent (1.7-fold) as observed for the same concentration of exogenously added 25-OHC and reached almost the level of transmigrated cells observed in the presence of FCS (Fig. 6). This increase was abrogated in both experimental settings in response to PTX, an inhibitor of the α_i subunits of G protein-coupled receptors.

Silencing of EBI2 reduces THP-1 migration in response to 25-OHC

EBI2, a G protein-coupled receptor that directs immune cell migration in response to oxysterols [29,30], is expressed in monocytes [41]. Thus it is likely that EBI2 could mediate pro-migratory effects on THP-1 monocytes in response to 25-OHC. Using a siRNA approach, silencing efficiency of EBI2 was first analyzed on mRNA and protein level. On mRNA level EBI2 was decreased by 83% and 68% (24 h and 48 h post silencing) in response to siRNA transfection. On protein level THP-1 monocytes express EBI2 under basal conditions (Fig. 7A). Mock transfection slightly increased EBI2 protein expression, whereas scrambled siRNA was without pronounced effects. Silencing of EBI2 resulted in an approx. 60% reduction (in comparison to scrambled siRNA) of EBI2 on protein level as calculated by densitometric analysis of immunoreactive bands (Fig. 7A). Next, migration experiments were performed in the presence of 25-OHC. Mock transfection reduced the number of transmigrated cells by 38%, scrambled siRNA by 55% and siEBI2 by 76% (Fig. 7B). Thus, in comparison to scrambled siRNA silencing of EBI2 results in a 46% reduction of migrated cells.

Discussion

Data obtained during the present study demonstrate that GBM cells express CH25H on mRNA and protein level in a cytokineinducible manner and are able to synthesize and secrete 25-OHC. Exogenously added 25-OHC and lipid extracts obtained from GM133 conditioned medium induced migration of THP-1 cells in an EBI2-dependent manner. Also primary human peripheral blood monocytes responded with increased migration to exogenously added 25-OHC. Thus GBM-derived 25-OHC is likely to act as a chemotactic signal that induces recruitment of monocytes towards tumor cells thereby contributing to the deposition of tumor-associated macrophages.

Macrophages and dendritic cells respond to Toll-like receptor (TLR) ligands by upregulating CH25H expression [4,5]. In the latter cell type TLR-dependent upregulation is mediated via a signalling pathway that involves NFκB and IFNβ secretion and converges on activation of the JAK/STAT1 pathway [4]. In vivo, exposure of mice to the selective TLR4 agonist KDO induced strong upregulation of CH25H in brain [26]. Results of the present study revealed upregulated CH25H transcription and translation in GBM cells. Interestingly, within the NCI60 data set contained in the BioGPS gene portal GBM cells appear to take a unique role in terms of highest CH25H expression (http://biogps.org). The response to TNFα and IL1β was different with respect to cytokine selectivity in the two cell lines studied here (Fig. 1). Whether this is due to different cytokine receptor expression levels is currently not clear. However, both cytokines used here may activate JAK/STAT pathways. TNFα activates JAK/STAT1 [42] and IL1β activates STAT1 [43] and a STAT-like factor, leading to activation of gene transcription [44]. Therefore our observations are compatible with a pathway inducing transcriptional activation of CH25H identified in dendritic cells and macrophages [4].

In line with findings reported for lipopolysaccharide activated macrophages [5] we have observed efficient secretion of 25-OHC into the cellular supernatant. In experiments analyzing free transfer of cholesterol or 25-OHC from erythrocytes and plasma, exchange of

25-OHC was found to occur about 2000 times faster than that of cholesterol [45]. The rate of transfer of oxysterols from a monolayer to acceptor particles followed a clear rank order with the highest rate of transfer observed for 25-OHC [46]. As reported for the quantitatively dominating oxysterols 24S- and 27-OHC, also 25-OHC is transported in association with circulating lipoproteins including high-density lipoproteins [47]. This might be of functional importance for gliomagenesis since high-density lipoproteins containing sphingosine-1-phosphate (a potent lipid GBM mitogen; [48]) induced increased DNA synthesis, ERK phosphorylation and Ca^{2+} mobilization in glioma cells [49].

Significant progress has been made in elucidating the functional significance of oxysterol-induced B- and T-cell migration in lymphoid organs [29,30,50–52]. It is now widely accepted that EBI2-mediated chemotaxis represents an important molecular mechanism directing follicular B cell migration and localization. Of note, oxysterols represent natural ligands for EBI2 activation [29,30,51]. In line with findings from the present study (Fig. 6), PTX suppressed 7α,25-OHC stimulated and EBI2-mediated binding of GTP [30]. However, PTX-insensitive ERK activation in response to EBI2 engagement was also reported [52]. The functional potency of different oxysterols towards EBI2 is 7α,25-OHC>7α,27-OHC>7α–OHC>25-OHC>27-OHC [50]. Of relevance for the present study 25-OHC also confers agonist activity towards EBI2 albeit with lower affinity [32,33]. In line, silencing of EBI2 using 21-mer siRNA reduced 25-OHC-induced THP-1 migration by 46% (Fig. 7). Whether EBI2 is responsible for increased migration of primary human monocytes in response to 25-OHC remains to be elucidated. The reason why mock transfection (GeneMute) and transfection with scrambled siRNA reduced migration of THP-1 cells in response to 25-OHC is currently not clear. However, lipid-based transfection reagents impact on cellular phospholipid composition (enrichment in 16:0 or 22:6-containing phosphatidylcholine species; unpublished observation; S.F.), alterations that could account for different receptor responsiveness.

To get an indication whether GBM-derived 25-OHC could act as a chemotactic signal for monocytes, lipid extracts of GM133 media were used in THP-1 migration assays. Although an indirect approach, these experiments revealed that medium lipid extracts induced monocyte migration in a quantitatively comparable manner as identical concentrations of exogenously added 25-OHC (Fig. 6). A question remaining is how 25-OHC contributes to monocyte attraction in the tumor environment. Association of secreted 25-OHC with lipoproteins would be a plausible explanation. In light of the facts that HDL particles transport 25-OHC in the circulation [47], shuttle oxysterols between the circulation and the brain [2] and are potent effectors of the monocytic migratory response [53] this hypothesis could be reasonable. Silva and colleagues [54] showed that an oxysterol-containing lipid fraction isolated from osteoblast-conditioned medium potently induces migration of human breast cancer cells, raising the possibility that oxysterols even contribute to metastasis.

Results of the present study demonstrate that 25-OHC treatment of THP-1 monocytes induced vimentin intermediate filament reorganization to more cortical structures and a polarized phenotype (Fig. 5). Vimentin is the major intermediate filament protein present in leukocytes and plays an important role in leukocyte motility and endothelial diapedesis [55]. In line, vimentin intermediate filaments play a crucial role during adhesion molecule

assembly that is needed during attachment and transendothelial migration [56], an event accompanying the recruitment of circulating monocytes across the tumor vasculature [57]. A characterization of human glioblastoma-associated macrophages revealed that besides lymphocytes and microglia, monocytes/macrophages represent the dominating inflammatory cell population infiltrating these tumors [58].

In summary, data obtained during the present study make it attractive to hypothesize that GBM-derived 25-OHC is able to recruit EBI2-expressing immune cells to the tumor environment. Thereby, 25-OHC may contribute to the recruitment of tumor-associated monocytes/macrophages that are potent modulators of gliomagenesis [59].

Acknowledgments

Financial support was provided by the Austrian Nationalbank (Anniversary Fund, project number 14534), the Austrian Research Promotion Agency (FFG; grant No. Bridge P820107), and the Austrian Science Fund (FWF; grant No. F3007, DK-W1241 and W1226, and P22521) and the National Institutes of Neurological Disease and Stroke (NS73831 to PSM). We thank David W. Russell, University of Texas Southwestern Medical Center, Dallas, Texas, USA, for the monoclonal antibody directed against cholesterol 25-hydroxylase.

REFERENCES

[1]. Jusakul A, Yongvanit P, Loilome W, Namwat N, Kuver R. Mechanisms of oxysterol-induced carcinogenesis. Lipids Health Dis. 2011; 10:44. [PubMed: 21388551]

[2]. Bjorkhem I, Meaney S. Brain cholesterol: long secret life behind a barrier. Arterioscler. Thromb. Vasc. Biol. 2004; 24:806–815. [PubMed: 14764421]

[3]. Wang Y, Muneton S, Sjovall J, Jovanovic JN, Griffiths WJ. The effect of 24S-hydroxycholesterol on cholesterol homeostasis in neurons: quantitative changes to the cortical neuron proteome. J. Proteome Res. 2008; 7:1606–1614. [PubMed: 18303831]

[4]. Park K, Scott AL. Cholesterol 25-hydroxylase production by dendritic cells and macrophages is regulated by type I interferons. J. Leukoc. Biol. 2010; 88:1081–1087. [PubMed: 20699362]

[5]. Diczfalusy U, Olofsson KE, Carlsson AM, Gong M, Golenbock DT, Rooyackers O, Flaring U, Bjorkbacka H. Marked upregulation of cholesterol 25-hydroxylase expression by lipopolysaccharide. J. Lipid Res. 2009; 50:2258–2264. [PubMed: 19502589]

[6]. Villablanca EJ, Raccosta L, Zhou D, Fontana R, Maggioni D, Negro A, Sanvito F, Ponzoni M, Valentinis B, Bregni M, Prinetti A, Steffensen KR, Sonnino S, Gustafsson JA, Doglioni C, Bordignon C, Traversari C, Russo V. Tumor-mediated liver X receptor-alpha activation inhibits CC chemokine receptor-7 expression on dendritic cells and dampens antitumor responses. Nat. Med. 2010; 16:98–105. [PubMed: 20037595]

[7]. Traversari C, Russo V. Control of the immune system by oxysterols and cancer development. Curr. Opin. Pharmacol. 2012; 12:729–735. [PubMed: 22832233]

[8]. Repa JJ, Li H, Frank-Cannon TC, Valasek MA, Turley SD, Tansey MG, Dietschy JM. Liver X receptor activation enhances cholesterol loss from the brain, decreases neuroinflammation, and increases survival of the NPC1 mouse. J.Neurosci. 2007; 27:14470–14480. [PubMed: 18160655]

[9]. Waltl S, Patankar JV, Fauler G, Nusshold C, Ullen A, Eibinger G, Wintersperger A, Kratky D, Malle E, Sattler W. 25-Hydroxycholesterol regulates cholesterol homeostasis in the murine CATH.a neuronal cell line. Neurosci. Lett. 2013; 539:16–21. [PubMed: 23347841]

[10]. Laffitte BA, Repa JJ, Joseph SB, Wilpitz DC, Kast HR, Mangelsdorf DJ, Tontonoz P. LXRs control lipid-inducible expression of the apolipoprotein E gene in macrophages and adipocytes. Proc. Nat. Acad Sci. U.S.A. 2001; 98:507–512.

[11]. Tam SP, Ramharack R. The effect of 25-hydroxycholesterol on the regulation of apolipoprotein E mRNA levels and secretion in the human hepatoma HepG2. Atherosclerosis. 1992; 95:137–146. [PubMed: 1329783]

[12]. Brahimi F, Bertrand P, Starck M, Galteau MM, Siest G. Control of apolipoprotein E secretion in the human hepatoma cell line KYN-2. Cell Biochem. Funct. 2001; 19:51–58. [PubMed: 11223871]

[13]. Makoukji J, Shackleford G, Meffre D, Grenier J, Liere P, Lobaccaro JM, Schumacher M, Massaad C. Interplay between LXR and Wnt/beta-catenin signaling in the negative regulation of peripheral myelin genes by oxysterols. J. Neurosci. 2011; 31:9620–9629. [PubMed: 21715627]

[14]. Guo D, Reinitz F, Youssef M, Hong C, Nathanson D, Akhavan D, Kuga D, Amzajerdi AN, Soto H, Zhu S, Babic I, Tanaka K, Dang J, Iwanami A, Gini B, Dejesus J, Lisiero DD, Huang TT, Prins RM, Wen PY, Robins HI, Prados MD, Deangelis LM, Mellinghoff IK, Mehta MP, James CD, Chakravarti A, Cloughesy TF, Tontonoz P, Mischel PS. An LXR agonist promotes GBM cell death through inhibition of an EGFR/AKT/SREBP-1/LDLR-dependent pathway. Cancer Discov. 2011; 1:442–456. [PubMed: 22059152]

[15]. Chuu CP, Lin HP. Antiproliferative effect of LXR agonists T0901317 and 22(R)-hydroxycholesterol on multiple human cancer cell lines. Anticancer Res. 2010; 30:3643–3648. [PubMed: 20944148]

[16]. Fukuchi J, Kokontis JM, Hiipakka RA, Chuu CP, Liao S. Antiproliferative effect of liver X receptor agonists on LNCaP human prostate cancer cells. Cancer Res. 2004; 64:7686–7689. [PubMed: 15520170]

[17]. Chuu CP, Hiipakka RA, Kokontis JM, Fukuchi J, Chen RY, Liao S. Inhibition of tumor growth and progression of LNCaP prostate cancer cells in athymic mice by androgen and liver X receptor agonist. Cancer Res. 2006; 66:6482–6486. [PubMed: 16818617]

[18]. Chuu CP. Modulation of liver X receptor signaling as a prevention and therapy for colon cancer. Med. Hypotheses. 2011; 76:697–699. [PubMed: 21333456]

[19]. Goldstein JL, DeBose-Boyd RA, Brown MS. Protein sensors for membrane sterols. Cell. 2006; 124:35–46. [PubMed: 16413480]

[20]. Nachtergaele S, Mydock LK, Krishnan K, Rammohan J, Schlesinger PH, Covey DF, Rohatgi R. Oxysterols are allosteric activators of the oncoprotein Smoothened. Nat. Chem. Biol. 2012; 8:211–220. [PubMed: 22231273]

[21]. Corcoran RB, Scott MP. Oxysterols stimulate Sonic hedgehog signal transduction and proliferation of medulloblastoma cells. Proc. Nat. Acad. Sci. U.S.A. 2006; 103:8408–8413.

[22]. Xu L, Shen S, Ma Y, Kim JK, Rodriguez-Agudo D, Heuman DM, Hylemon PB, Pandak WM, Ren S. 25-Hydroxycholesterol-3-sulfate (25HC3S) attenuates inflammatory response via PPAR-gamma signaling in human THP-1 macrophages. Am. J. Physiol. Endocrinol. Metab. 2012; 302:E788–799. [PubMed: 22275753]

[23]. Russo V. Metabolism, LXR/LXR ligands, and tumor immune escape. J. Leukoc. Biol. 2011; 90:673–679. [PubMed: 21771899]

[24]. Stupp R, Hegi ME, van den Bent MJ, Mason WP, Weller M, Mirimanoff RO, Cairncross JG. Changing paradigms—an update on the multidisciplinary management of malignant glioma. Oncologist. 2006; 11:165–180. [PubMed: 16476837]

[25]. Guo D, Hildebrandt IJ, Prins RM, Soto H, Mazzotta MM, Dang J, Czernin J, Shyy JY, Watson AD, Phelps M, Radu CG, Cloughesy TF, Mischel PS. The AMPK agonist AICAR inhibits the growth of EGFRvIII-expressing glioblastomas by inhibiting lipo-genesis. Proc. Nat. Acad. Sci. U.S.A. 2009; 106:12932–12937.

[26]. Bauman DR, Bitmansour AD, McDonald JG, Thompson BM, Liang G, Russell DW. 25-Hydroxycholesterol secreted by macrophages in response to Toll-like receptor activation suppresses immunoglobulin A production. Proc. Nat. Acad. Sci. U.S.A. 2009; 106:16764–16769.

[27]. Liu Y, Hulten LM, Wiklund O. Macrophages isolated from human atherosclerotic plaques produce IL-8, and oxysterols may have a regulatory function for IL-8 production. Arterioscler. Thromb. Vasc. Biol. 1997; 17:317–323. [PubMed: 9081687]

[28]. Rydberg EK, Salomonsson L, Hulten LM, Noren K, Bondjers G, Wiklund O, Bjornheden T, Ohlsson BG. Hypoxia increases 25-hydroxycholesterol-induced interleukin-8 protein secretion in human macrophages. Atherosclerosis. 2003; 170:245–252. [PubMed: 14612204]

[29]. Hannedouche S, Zhang J, Yi T, Shen W, Nguyen D, Pereira JP, Guerini D, Baumgarten BU, Roggo S, Wen B, Knochenmuss R, Noel S, Gessier F, Kelly LM, Vanek M, Laurent S, Preuss I,

Miault C, Christen I, Karuna R, Li W, Koo DI, Suply T, Schmedt C, Peters EC, Falchetto R, Katopodis A, Spanka C, Roy MO, Detheux M, Chen YA, Schultz PG, Cho CY, Seuwen K, Cyster JG, Sailer AW. Oxysterols direct immune cell migration via EBI2. Nature. 2011; 475:524–527. [PubMed: 21796212]

[30]. Liu C, Yang XV, Wu J, Kuei C, Mani NS, Zhang L, Yu J, Sutton SW, Qin N, Banie H, Karlsson L, Sun S, Lovenberg TW. Oxysterols direct B-cell migration through EBI2. Nature. 2011; 475:519–523. [PubMed: 21796211]

[31]. Yeung YT, Bryce NS, Adams S, Braidy N, Konayagi M, McDonald KL, Teo C, Guillemin GJ, Grewal T, Munoz L. p38 MAPK inhibitors attenuate pro-inflammatory cytokine production and the invasiveness of human U251 glioblastoma cells. J. Neurooncol. 2012; 109:35–44. [PubMed: 22528800]

[32]. Sharma V, Dixit D, Koul N, Mehta VS, Sen E. Ras regulates interleukin-1beta-induced HIF-1alpha transcriptional activity in glioblastoma. J. Mol. Med. (Berl.). 2011; 89:123–136. [PubMed: 20865400]

[33]. Zhu VF, Yang J, Lebrun DG, Li M. Understanding the role of cytokines in glioblastoma multiforme pathogenesis. Cancer Lett. 2012; 316:139–150. [PubMed: 22075379]

[34]. Ye XZ, Xu SL, Xin YH, Yu SC, Ping YF, Chen L, Xiao HL, Wang B, Yi L, Wang QL, Jiang XF, Yang L, Zhang P, Qian C, Cui YH, Zhang X, Bian XW. Tumor-associated microglia/macrophages enhance the invasion of glioma stem-like cells via TGF-beta1 signaling pathway. J. Immunol. 2012; 189:444–453. [PubMed: 22664874]

[35]. Wang Y, Zhu S, Cloughesy TF, Liau LM, Mischel PS. p53 disruption profoundly alters the response of human glioblastoma cells to DNA topoisomerase I inhibition. Oncogene. 2004; 23:1283–1290. [PubMed: 14961077]

[36]. Pfaffl MW. A new mathematical model for relative quantification in real-time RT-PCR. Nucleic Acids Res. 2001; 29:e45. [PubMed: 11328886]

[37]. Folch J, Lees M, Sloane Stanley GH. A simple method for the isolation and purification of total lipides from animal tissues. J. Biol. Chem. 1957; 226:497–509. [PubMed: 13428781]

[38]. Fan H, Hall P, Santos LL, Gregory JL, Fingerle-Rowson G, Bucala R, Morand EF, Hickey MJ. Macrophage migration inhibitory factor and CD74 regulate macrophage chemotactic responses via MAPK and Rho GTPase. J. Immunol. 2011; 186:4915–4924. [PubMed: 21411731]

[39]. Ulcar R, Peskar BA, Schuligoi R, Heinemann A, Kessler HH, Santner BI, Amann R. Cyclooxygenase inhibition in human monocytes increases endotoxin-induced TNF alpha without affecting cyclooxygenase-2 expression. Eur. J. Pharmacol. 2004; 501:9–17. [PubMed: 15464057]

[40]. Baay M, Brouwer A, Pauwels P, Peeters M, Lardon F. Tumor cells and tumor-associated macrophages: secreted proteins as potential targets for therapy. Clin. Dev. Immunol. 2011:565187. [PubMed: 22162712]

[41]. Rosenkilde MM, Benned-Jensen T, Andersen H, Holst PJ, Kledal TN, Luttichau HR, Larsen JK, Christensen JP, Schwartz TW. Molecular pharmacological phenotyping of EBI2. An orphan seven-transmembrane receptor with constitutive activity. J. Biol. Chem. 2006; 281:13199–13208. [PubMed: 16540462]

[42]. Guo D, Dunbar JD, Yang CH, Pfeffer LM, Donner DB. Induction of Jak/STAT signaling by activation of the type 1 TNF receptor. J. Immunol. 1998; 160:2742–2750. [PubMed: 9510175]

[43]. Lee SH, Nishino M, Mazumdar T, Garcia GE, Galfione M, Lee FL, Lee CL, Liang A, Kim J, Feng L, Eissa NT, Lin SH, Yu-Lee LY. 16-kDa prolactin down-regulates inducible nitric oxide synthase expression through inhibition of the signal transducer and activator of transcription 1/IFN regulatory factor-1 pathway. Cancer Res. 2005; 65:7984–7992. [PubMed: 16140971]

[44]. Tsukada J, Waterman WR, Koyama Y, Webb AC, Auron PE. A novel STAT-like factor mediates lipopolysaccharide, interleukin 1 (IL-1), and IL-6 signaling and recognizes a gamma interferon activation site-like element in the IL1B gene. Mol. Cell Biol. 1996; 16:2183–2194. [PubMed: 8628285]

[45]. Lange Y, Ye J, Strebel F. Movement of 25-hydroxycholesterol from the plasma membrane to the rough endoplasmic reticulum in cultured hepatoma cells. J. Lipid Res. 1995; 36:1092–1097. [PubMed: 7658157]

[46]. Theunissen JJ, Jackson RL, Kempen HJ, Demel RA. Membrane properties of oxysterols. Interfacial orientation, influence on membrane permeability and redistribution between membranes. Biochim. Biophys. Acta. 1986; 860:66–74. [PubMed: 3730387]

[47]. Babiker A, Diczfalusy U. Transport of side-chain oxidized oxysterols in the human circulation. Biochim. Biophys. Acta. 1998; 1392:333–339. [PubMed: 9630709]

[48]. Van Brocklyn J, Letterle C, Snyder P, Prior T. Sphingosine-1-phosphate stimulates human glioma cell proliferation through Gi-coupled receptors: role of ERK MAP kinase and phosphatidylinositol 3-kinase beta. Cancer Lett. 2002; 181:195–204. [PubMed: 12175535]

[49]. Malchinkhuu E, Sato K, Muraki T, Ishikawa K, Kuwabara A, Okajima F. Assessment of the role of sphingosine 1-phosphate and its receptors in high-density lipoprotein-induced stimulation of astroglial cell function. Biochem. J. 2003; 370:817–827. [PubMed: 12470300]

[50]. Zhang L, Shih AY, Yang XV, Kuei C, Wu J, Deng X, Mani NS, Mirzadegan T, Sun S, Lovenberg TW, Liu C. Identification of structural motifs critical for epstein-barr virus-induced molecule 2 function and homology modeling of the ligand docking site. Mol. Pharmacol. 2012; 82:1094–1103. [PubMed: 22930711]

[51]. Yi T, Wang X, Kelly LM, An J, Xu Y, Sailer AW, Gustafsson JA, Russell DW, Cyster JG. Oxysterol gradient generation by lymphoid stromal cells guides activated B cell movement during humoral responses. Immunity. 2012; 37:535–548. [PubMed: 22999953]

[52]. Benned-Jensen T, Norn C, Laurent S, Madsen CM, Larsen HM, Arfelt KN, Wolf RM, Frimurer T, Sailer AW, Rosenkilde MM. Molecular characterization of oxysterol binding to the Epstein-Barr virus-induced gene 2 (GPR183). J. Biol. Chem. 2012; 287:35470–35483. [PubMed: 22875855]

[53]. Bursill CA, Castro ML, Beattie DT, Nakhla S, van der Vorst E, Heather AK, Barter PJ, Rye KA. High-density lipoproteins suppress chemokines and chemokine receptors in vitro and in vivo. Arterioscler. Thromb. Vasc. Biol. 2010; 30:1773–1778. [PubMed: 20702809]

[54]. Silva J, Beckedorf A, Bieberich E. Osteoblast-derived oxysterol is a migration-inducing factor for human breast cancer cells. J. Biol. Chem. 2003; 278:25376–25385. [PubMed: 12734199]

[55]. Ivaska J, Pallari HM, Nevo J, Eriksson JE. Novel functions of vimentin in cell adhesion, migration, and signaling. Exp. Cell Res. 2007; 313:2050–2062. [PubMed: 17512929]

[56]. Nieminen M, Henttinen T, Merinen M, Marttila-Ichihara F, Eriksson JE, Jalkanen S. Vimentin function in lymphocyte adhesion and transcellular migration. Nat. Cell Biol. 2006; 8:156–162. [PubMed: 16429129]

[57]. Schmid MC, Varner JA. Myeloid cells in tumor inflammation. Vasc. Cell. 2012; 4:14. [PubMed: 22938502]

[58]. Parney IF, Waldron JS, Parsa AT. Flow cytometry and in vitro analysis of human glioma-associated macrophages. J. Neurosurg. 2009; 110:572–582. [PubMed: 19199469]

[59]. Charles A, Holland EC, Gilbertson R, Glass R, Kettenmann H. The brain tumor microenvironment. Glia. 2011; 59:1169–1180. [PubMed: 21446047]

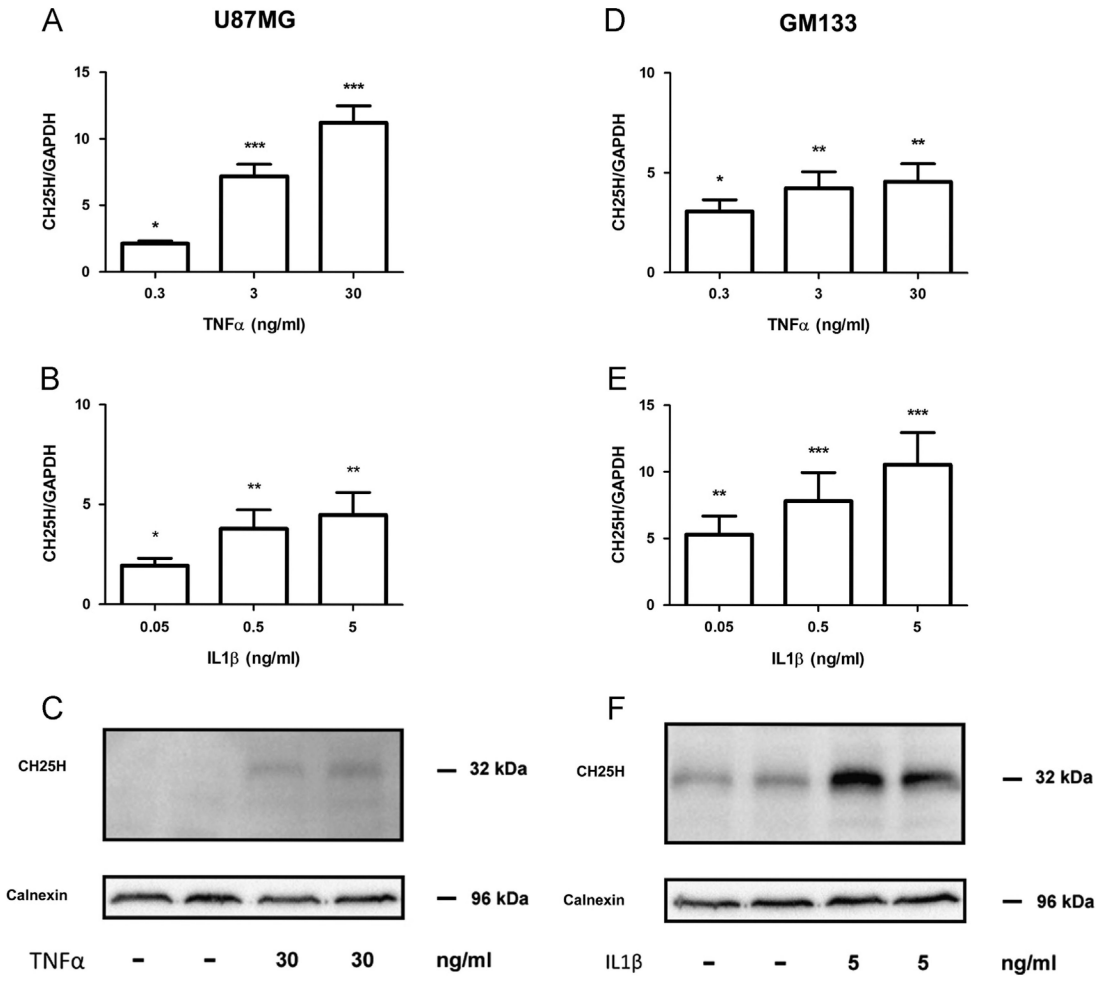

Fig. 1.

Exogenous TNFα and IL-1β increase CH25H mRNA and protein in U87MG and GM133 cells. Cells were cultured under standard conditions and incubated in the presence of the indicated TNFα or IL1β concentrations. Six hours post cytokine addition U87MG ((A), (B)) or GM133 ((D), (E)) cells were lysed, RNA was isolated, reverse transcribed and target gene expression was analyzed by qPCR. GAPDH was used as housekeeping gene. Gene expression ratios were calculated by REST and analysed by a pair wise fixed random reallocation test. Data are shown as mean±SD of 3 independent experiments. *p<0.05, **p<0.01, ***p<0.001. Twenty four hours post cytokine addition U87MG (C) or GM133 (F) cells were lysed and protein lysates (50 µg/lane) were separated by SDS-PAGE (12% gels) and electrophoretically transferred to PVDF membranes. CH25H (approx. 32 kDa) was detected with a monoclonal antibody. Bands were visualized using the ECL system. Calnexin (96 kDa) was used as loading control.

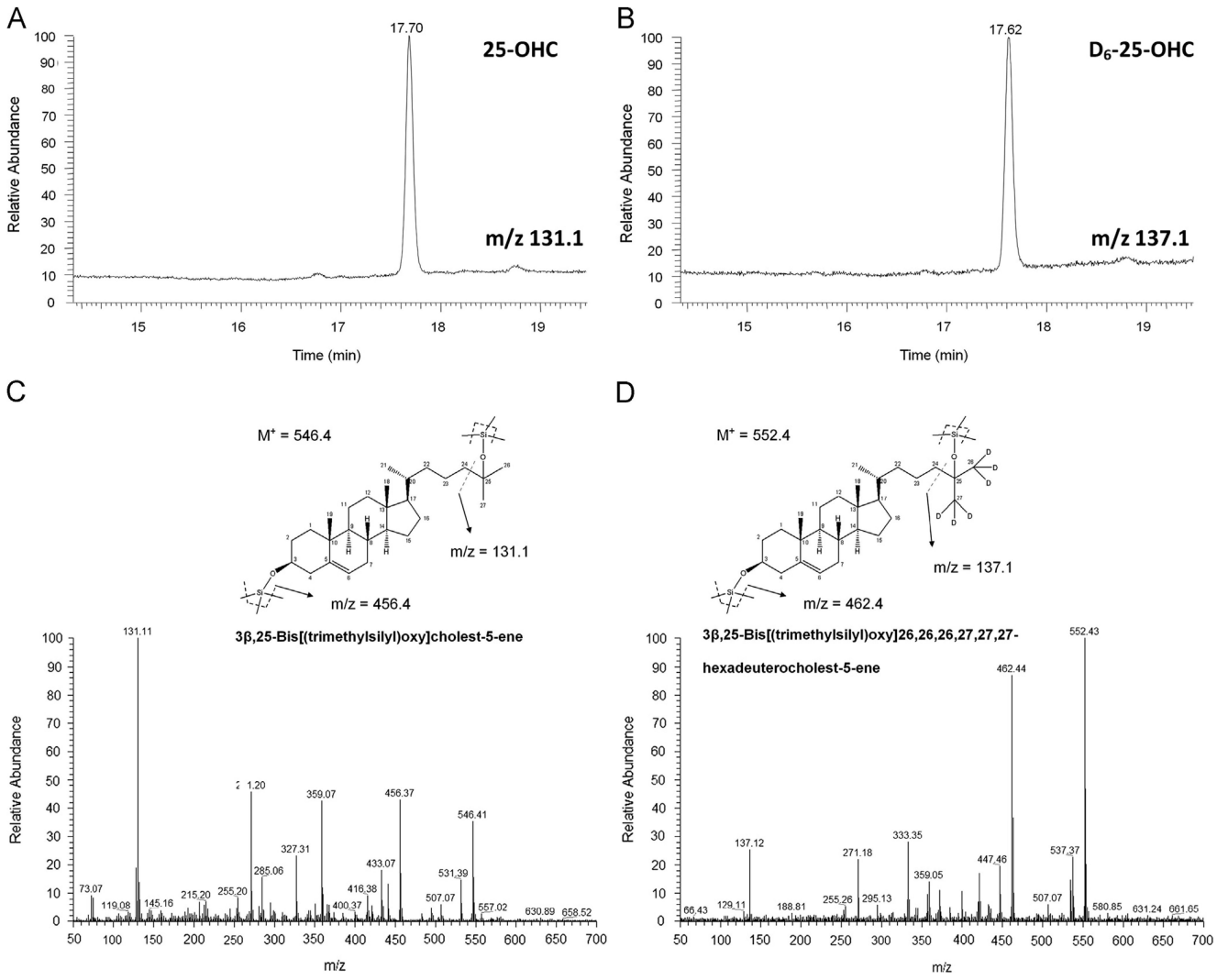

Fig. 2.

GC–MS analysis of 25-OHC-TMS derivatives. Selected ion chromatograms of (A) 25-OHC (*m/z*=131.1) and (B) D_6-25-OHC (*m/z*=137.1). Full scan EI spectra of 25-OHC and D_6-25-OHC are shown in (C) and (D), respectively. The proposed fragmentation patterns of both analytes are shown as insets.

Europe PMC Funders Author Manuscripts

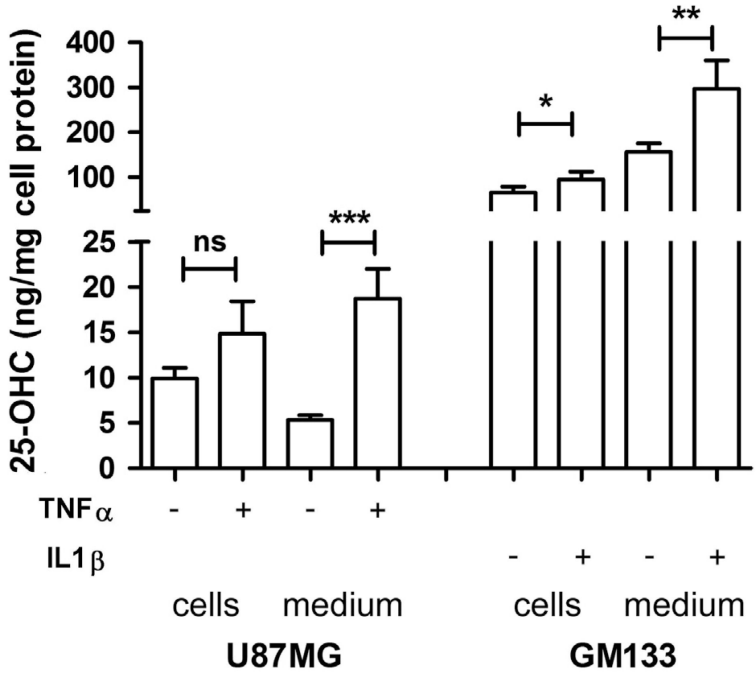

Fig. 3.

25-OHC synthesis and secretion by U87MG and GM133 is stimulated by cytokines. U87MG and GM133 cells were treated with the indicated concentrations of TNFα or IL1β (vehicle=1% BSA in PBS) for 24 h. Cellular and medium lipids were extracted, converted to the corresponding TMS derivatives and analysed by GC–MS. D_6-25-OHC was used as internal standard. Results were normalized to the cellular protein content and are expressed as mean±SD (n=3). Student's t-test was used to compare vehicle- vs. cytokine treated samples. *p<0.05, **p<0.01, ***p<0.001. ns = not significant.

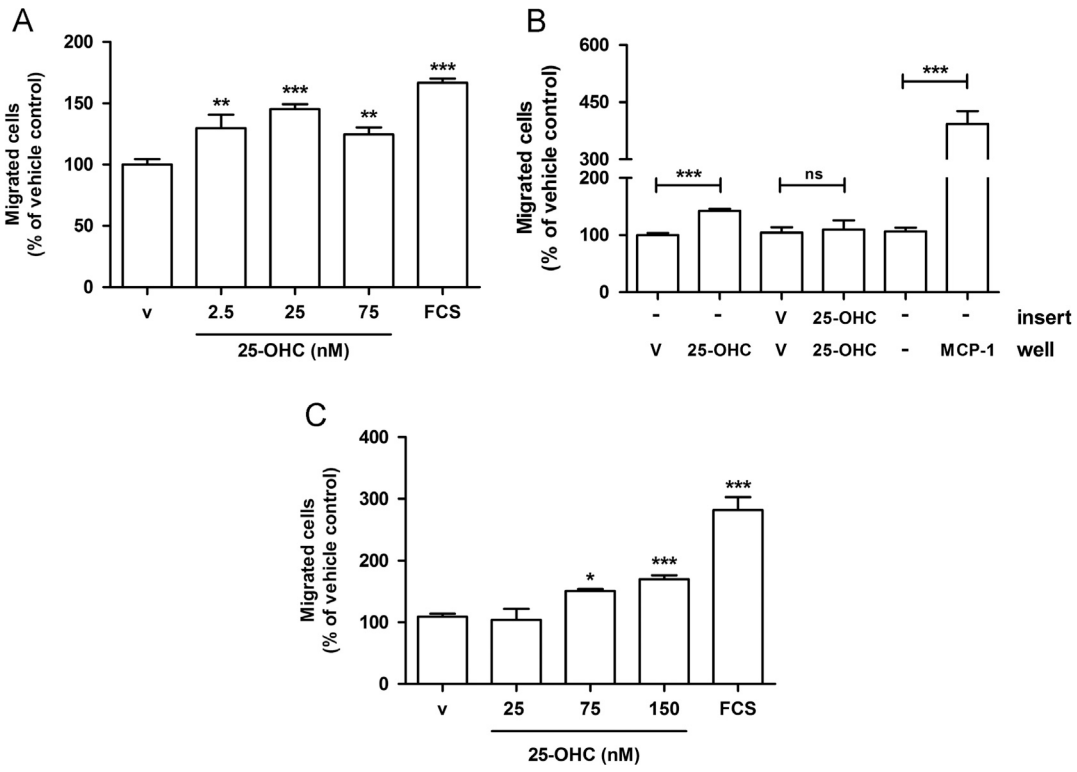

Fig. 4.

25-OHC induces migration of THP-1 cells and primary human monocytes. (A) THP-1 cells (100,000) were seeded into the upper chamber of uncoated Transwell chambers. The lower chamber was containing medium with vehicle ('v'; 0.1% ethanol), the indicated 25-OHC concentrations, or FCS (5%) as positive control for cell migration. After 18 h, transmigrated cells were counted. Migration into the lower chamber of the transwell of untreated cells (100%) was compared with that of cells exposed to 25-OHC or FCS added to the lower chamber. Results represent mean±SEM from three independent experiments and are expressed as % of vehicle control. (B) THP-1 cells (100,000) were seeded into the upper chamber of uncoated Transwell chambers. To differentiate between chemotactic and chemokinetic effects, 25 nM 25-OHC was added to the lower ('well') or to both, the lower and the upper ('insert') chamber. After 18 h, transmigrated cells were counted. Migration towards 50 ng/ml MCP-1 was used as positive control. Results represent mean±SEM from two independent experiments and are expressed as % of the corresponding vehicle controls. (C) Human peripheral blood monocytes (500,000) were seeded into the upper Transwell chambers. After 4 h transmigrated cells in the lower compartment were counted. Data shown represent mean±SEM of two independent experiments and are expressed as % of vehicle control. ((A), (C)): One-way ANOVA with Bonferroni multiple comparison test or (B) Students *t*-test. **p*<0.05, ***p*<0.01, ****p*<0.001. ns = not significant.

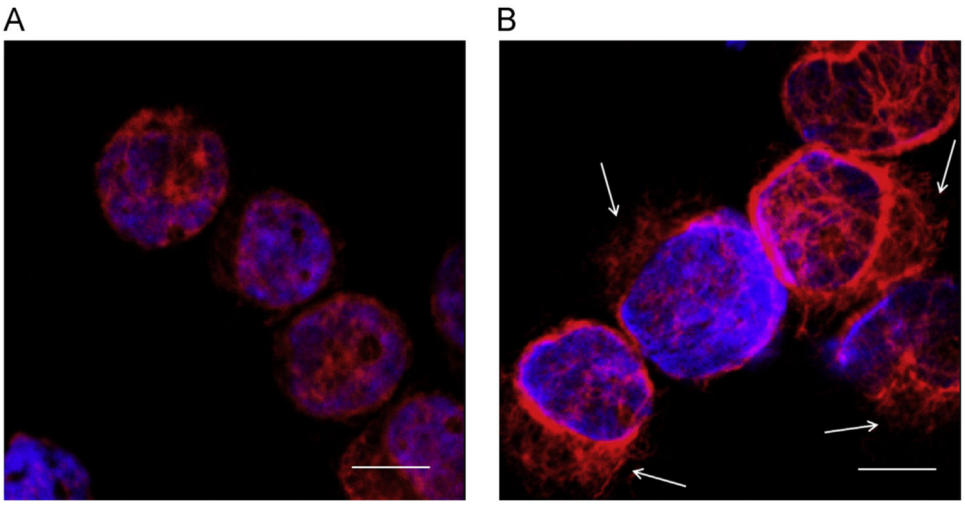

Fig. 5.

25-OHC induces reorganization of vimentin in THP-1 cells. THP-1 cells were treated with vehicle (A) or 25-OHC (25 nM, 18 h; (B)), fixed with acetone, and vimentin was immunostained with mouse anti-human vimentin and a Cy3-labeled anti-mouse IgG. Nuclei were counterstained with DAPI. The bar indicates 10 μm. Arrows indicate areas of vimentin intermediate filament polarization.

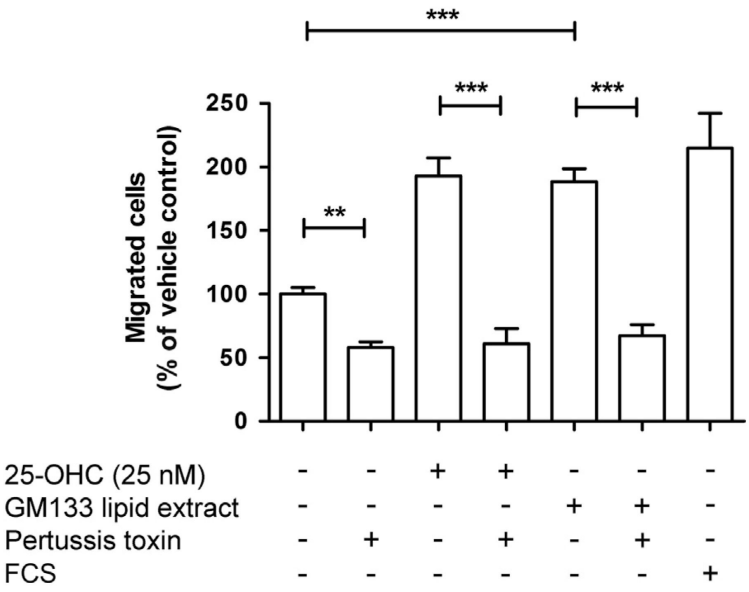

Fig. 6.

Lipid extracts from GM133 conditioned medium induce THP-1 migration via a pertussis toxin-sensitive pathway. THP-1 cells (100,000) were seeded into the upper chamber of Transwell chambers. The lower chamber contained medium with vehicle (0.1% ethanol), 25-OHC, GM133-conditioned medium lipid extracts (0.5 µl of reconstituted lipid extracts in ethanol was added to the medium to result in a 25-OHC concentration of approx. 25 nM), or FCS in the absence or presence of PTX (30 ng/ml). After 18 h, transmigrated cells were counted. Cell numbers are expressed as % of the vehicle control. Results represent mean ±SEM of three independent experiments. One-way ANOVA with Bonferroni multiple comparison test was used. $^{**}p<0.01$, $^{***}p<0.001$.

Europe PMC Funders Author Manuscripts

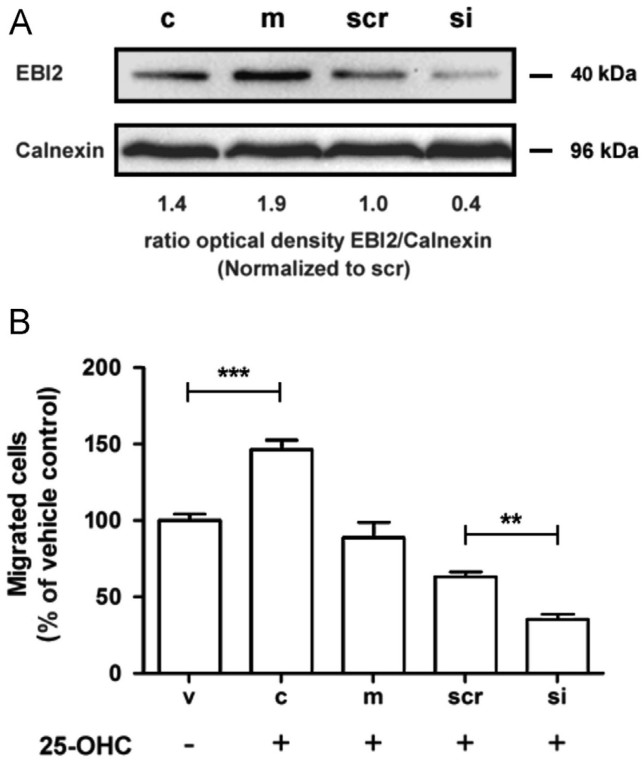

Fig. 7.

Silencing of the oxysterol receptor EBI2 reduces THP-1 migration in response to 25-OHC. (A) THP-1 cells were cultured under standard conditions and were either mock transfected or transfected with non-targeting and EBI-2 siRNA. After 72 h, cells were lysed and protein extracts (150 μg) were separated by SDS-PAGE (12%) and electrophoretically transferred to a PVDF membrane. EBI2 (40 kDa) was detected with a polyclonal antibody. Immunoreactive bands were visualized using the ECL system. (B) THP-1 cells (100,000) of each group (v=vehicle-treated; c=untransfected control; m=mock, scr=scrambled and si=EBI2 siRNA transfected cells) were seeded into the upper chamber of Transwell chambers, the lower chamber (except vehicle controls; only 0.1% ethanol) contained 25-OHC (25 nM). After 18 h transmigrated cells were counted. The migration experiment started 48 h after siRNA transfection. Data shown represent mean±SEM of 3 independent experiments. One-way ANOVA with Bonferroni multiple comparison test was used. $^{**}p<0.01$, $^{***}p<0.001$.

Europe PMC Funders Author Manuscripts